# Fast non-Cartesian $L_1$-SPIRiT with Field Inhomogeneity Correction

Daniel S. Weller[1] and Jeffrey A. Fessler[1]
[1]*EECS, University of Michigan, Ann Arbor, MI, United States*

**Introduction** Recently, a fast algorithm[1] was presented for $L_1$-SPIRiT[2-4] reconstruction of non-Cartesian undersampled multi-channel k-space data. Single-shot non-Cartesian pulse sequences, combined with parallel imaging, can acquire k-space very quickly. However, the relatively long readouts of such sequences introduce artifacts due to $B_0$ inhomogeneity and $R_2^*$ effects. Using existing methods for estimating field maps[5], we extend the fast non-Cartesian $L_1$-SPIRiT method[1] by incorporating $B_0$ and $R_2^*$ effects into the system model. Using simulated and real phantom data, we demonstrate that our method effectively mitigates field inhomogeneity artifacts.

**Theory** The cost function for non-Cartesian $L_1$-SPIRiT is $\arg\min_{\mathbf{x}} \frac{1}{2}\|\mathbf{Ax}-\mathbf{d}\|_2^2 + \frac{\lambda}{2}\|\mathbf{Gx}-\mathbf{x}\|_2^2 + \gamma_1\|\mathbf{\Psi x}\|_{1,2} + \gamma_2\|\mathbf{Cx}\|_{1,2}$ , where **x** is the set of multi-channel images, **A** is the system matrix implemented using the nonuniform fast Fourier transform (NUFFT)[6], **d** is the k-space data, **G** is the SPIRiT operator, **Ψ** and **C** are wavelet and finite-differences transforms, respectively, the $\|\cdot\|_{1,2}$-norm encourages joint sparsity across the coils, and $\lambda$, $\gamma_1$, and $\gamma_2$ are tuning parameters. In this work, we augment the system matrix **A** with histogram-based time segmentation[7] to account for $B_0$ inhomogeneity and $R_2^*$ relaxation. We define auxiliary split variables $\mathbf{z} = \mathbf{x}$, $\mathbf{w} = \mathbf{\Psi x}$, and $\mathbf{g}_{xy} = \mathbf{Cx}$, and use the alternating directions method of multipliers (ADMM)[8]. The ADMM subproblems are the same as in the earlier algorithm[1], using the new system matrix **A** in the subproblem minimizing **x**. The Hessian matrix for the **x**-update step is $\mathbf{H_x} = \mathbf{A'A} + \mu_1\mathbf{I} + \mu_2\mathbf{\Psi'\Psi} + \mu_2\mathbf{C'C}$, where $\mu_1$, $\mu_2$ are ADMM penalty parameters. By design, **Ψ** and **C** have circulant Gram matrices. In the original problem, the matrix **A'A** was nearly circulant (Toeplitz), but the spatially varying $B_0$ and $R_2^*$ effects destroy this structure. Nevertheless, we employ a circulant preconditioner **P** for this problem. We design this preconditioner by first finding the response $\mathbf{H_A}$ of **A'A** to a centered unit impulse. Because $\mathbf{H_A}$ may have negative eigenvalues, and may not be a good surrogate for **A'A**, we find $\alpha, \beta > 0$ that minimizes $\alpha\|\mathbf{H_A}+\beta\mathbf{I}\|_F$ while satisfying $\mathbf{H_A}+\beta\mathbf{I} \geq 0$, and $\alpha(\mathbf{H_A}+\beta\mathbf{I}) \geq \mathbf{A'A}$. Then, $\mathbf{P} = [\alpha(\mathbf{H_A}+\beta\mathbf{I}) + \mu_1\mathbf{I} + \mu_2\mathbf{\Psi'\Psi} + \mu_2\mathbf{C'C}]^{-1}$. We calibrate tuning parameters using condition numbers[1], approximating the eigenvalues of **A'A** with those of $\mathbf{H_A}$.

**Methods** We simulated a $T_1$-weighted slice from Brainweb[9] with an interleaved spiral-out trajectory (3 leaves with 5485 points/leaf, 128×128 matrix size) using an eight-channel simulated coil in the presence of both $R_2^*$ decay and $B_0$ inhomogeneity maps from the Image Reconstruction toolbox[10]. Sampling k-space, coil sensitivities, and field maps were applied to a 512×512 high-resolution image, including subvoxel effects, and the acquired data were reconstructed at 128×128 resolution. We used a 30×30 Cartesian k-space region for calibrating 7×7 SPIRiT kernels. The system matrix was computed using L=8 time segments from 128×128 low-resolution field maps. We retained one spiral leaf and added 40 dB signal-to-noise ratio (SNR) complex Gaussian noise (correlated across coil channels) for reconstruction. We reconstructed the simulated k-space data using our method and the existing non-Cartesian $L_1$-SPIRiT algorithm[1]. The original image at the reconstructed resolution served as the ground truth for this experiment.

In the second experiment, we imaged an ACR phantom using an eight-channel receive array head coil in a 3 T GE Discovery MRI scanner. First, we acquired 14 slices (each 3 mm thick) with 20 cm FOV (128x128 matrix size) using a 3-D Cartesian spin warp pulse sequence (TR = 33 ms, 12° flip) for four different echo times (TE = 5.12, 7.12, 9.12, 11.1 ms) and generated $B_0$ maps for each slice via regularized field map estimation[5]; we incorporated the resulting field maps into our system model using L = 8 time segments. Then we collected a 3-shot (per slice-encode) interleaved 3-D stack-of-spirals trajectory (TR = 250 ms, TE = 9.68 ms, 30° flip) with the same volume prescription as the Cartesian scans; we used just one leaf for reconstruction. We also averaged five acquisitions of a 30-shot interleaved 3-D stack-of-spirals trajectory with the same parameters to use as a ground truth. In both experiments, conjugate phase images were used to initialize both methods, and both methods were run for the same amount of time (60 s).

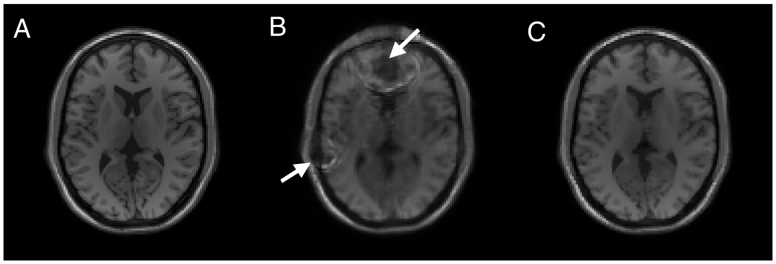

Fig. 1: Compared to the (A) ground truth Brainweb image, the non-Cartesian $L_1$-SPIRiT reconstruction (B) without field inhomogeneity correction[1] shows artifacts, especially in the frontal and lateral regions (arrows). The (C) proposed method appears free of these effects. The images shown result from 60 s of reconstruction time.

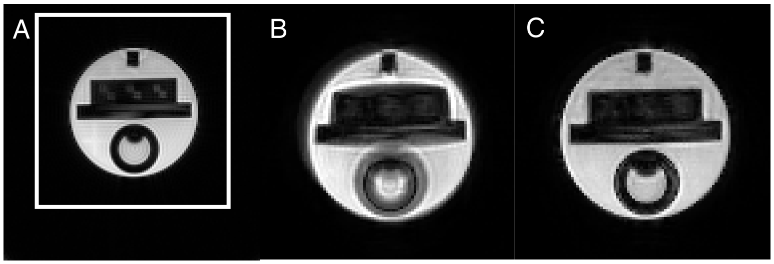

Fig. 2: The (A) 30-shot spiral ACR phantom ground truth is free of the geometric distortions and blurring caused by field inhomogeneity present in the (B) image reconstructed using the existing method[1] on single-shot spiral data. The (C) image reconstructed using our proposed method is much closer to the ground truth. Both (B) and (C) were obtained from 60 s of reconstruction time. The inset region in (A) is enlarged in (B) and (C) to reveal detail.

**Results** Fig. 1 portrays sum-of-squares combined images for the Brainweb experiment. Normalized root mean squared error (NRMSE) values for the complex coil non-Cartesian $L_1$-SPIRiT reconstructions, without and with field inhomogeneity correction, are 95% and 8.7%, respectively. Magnitude NRMSE values are 21% and 8.1%. Computation time for the proposed method increased from 0.24±0.03 s/iteration to 0.83±0.03 s/iteration. Fig. 2 displays ACR phantom magnitude images. Visible artifacts, especially geometric distortions and blurring, are clearly reduced after 60 s of reconstruction time in both experiments.

**Discussion** The reconstructed images and NRMSE values corroborate the hypothesis that incorporating $B_0$ and $R_2^*$ effects into $L_1$-SPIRiT effectively reduces the artifacts that would otherwise discourage using sequences with long readout times. Dynamic and functional acquisitions, where repetition time, spatial resolution, and SNR are all important, can benefit from this technique that produces high-resolution, high-quality images quickly from undersampled data. While field maps may be time-consuming to acquire, they may be measured just once and reused throughout a dynamic sequence. Since the NUFFT's, SPIRiT operators, and transforms are highly parallel, a fast implementation of our proposed method on a graphical processing unit may be suitable for real time reconstructions.

**Acknowledgments** The authors thank Jon-Fredrik Nielsen for assistance acquiring phantom data and NIH F32 EB015914 and NIH/NCI P01 CA87634.

**References** 1. Weller DS, Ramani S, Fessler JA. IEEE Trans Med Imag. 2013; in press. 2. Lustig M, Alley M, Vasanawala S, et al. Proc ISMRM. 2009; p. 334. 3. Lustig M, Pauly JM. Mag Res Med. 2010;64(2): 457-71. 4. Murphy M, Alley M, Demmel J, et al. IEEE Trans Med Imag. 2012;31(6): 1250-62. 5. Funai AK, Fessler JA, Yeo DTB, et al. IEEE Trans Med Imag. 2008;27(10): 1484-94. 6. Fessler JA, Sutton BP. IEEE Trans Sig Proc. 2003;51(2): 560-74. 7. Fessler JA, Lee S, Olafsson VT, et al. IEEE Trans Sig Proc. 2005;53(9): 3393-402. 8. Glowinski R, Marrocco A. Inf Rech Oper. 1975;R-2: 41-76. 9. Kwan RKS, Evans AC, Pike GB. IEEE Trans Med Imag. 1999;18(11): 1085-97. 10. Available http://web.eecs.umich.edu/~fessler/code/index.html.